International Journal of Heat and Mass Transfer 51 (2008) 5617–5622

Contents lists available at ScienceDirect

International Journal of Heat and Mass Transfer

journal homepage: www.elsevier.com/locate/ijhmt

Temperature considerations during irreversible electroporation

Rafael V. Davalos [a,*], Boris Rubinsky [b,c]

[a] School of Biomedical Engineering and Sciences, Virginia Tech-Wake Forest University, Blacksburg, VA 24061, USA
[b] Department of Bioengineering, Department of Mechanical Engineering and Graduate Program in Biophysics, University of California at Berkeley, Berkeley, CA 94720, USA
[c] Center for Bioengineering in the Service of Humanity and Society, School of Computer Science and Engineering, Hebrew University of Jerusalem, Givat Ram, Jerusalem 91904, Israel

ARTICLE INFO

Article history:
Received 19 November 2007
Received in revised form 4 April 2008
Available online 14 June 2008

Keywords:
Cell membrane
Irreversible electroporation
Tissue ablation
Oncology

ABSTRACT

Certain electrical fields, when applied across a cell membrane, can have the sole effect of membrane permeabilization, which is referred to as electroporation. When the permeabilization is irreversible, the effect leads to cell death, primarily due to loss of cell homeostasis, in a process known as irreversible electroporation (IRE). This is an unusual mode of cell death that is not yet fully understood. However, it is unique among tissue ablation techniques in affecting only the cell membrane while tissue molecules, everything encompassing collagen structures to proteins, remain intact. This facilitates a possible immune response and avoids scar tissue formation. Irreversible electroporation is, therefore, substantially different from any other tissue ablation technique and has many advantages over either heating or freezing thermal ablation. However, since IRE employs electrical fields, it can produce thermal effects which could cause thermal damage if parameters are not chosen correctly, therapy negating the advantages of IRE. This study evaluates the temperature distribution during typical IRE protocols as a means to establish the electrical parameters that produce IRE alone, without thermal effects.

1. Introduction

Certain electrical fields, when applied across a cell, have the ability to permeabilize the cell membrane through a process that was named in the early 1980's "electroporation" [1]. The mechanism through which the cell membrane is permeabilized is not yet fully understood. It is thought to be related to the formation of nano-scale defects or pores in the cell membrane, from which the term "poration" was derived. When electrical fields permeabilize the cell membrane temporarily after which the cells survive, the process is known as "reversible electroporation". Other fields can cause the cell membrane to become permanently permeabilized, after which the cells die, in a process referred to as "irreversible electroporation".

Reversible electroporation has become an important tool in biotechnology and medicine. Among the many uses are the permeabilization of the cell membrane to molecules that normally do not penetrate the membrane [1], fusion of cells [2], introduction of drugs into cells [3,4], electrochemotherapy for treatment of cancer [5], gene delivery in tissue [6], and transdermal delivery of drugs and genes. Numerous reviews, books, issues of journals and thousands of publications were published on the various features of reversible electroporation, such as [7–16].

The various applications of reversible electroporation require cells to survive the procedure. Therefore, the occurrence of irreversible electroporation, in which cells die, is obviously undesirable [17]. During the last three decades, the field of electroporation has been dominated by reversible electroporation applications. Irreversible electroporation was viewed as an undesirable side effect and was studied only to define the upper limit of electrical parameters that induce reversible electroporation. However, during the last few years, irreversible electroporation has begun to emerge as an important minimally invasive ablation technique in its own right [18].

It is not disputed that every electrical field, including a field for IRE, produces a thermal effect, the so-called Joule effect. It is also indisputable that certain electrical fields can produce irreversible electroporation. The question that was raised in an analytical study by Davalos et al. is whether irreversible electroporation can be isolated from thermal effects and used by itself to produce substantial volumes of tissue ablation *in vivo*, with negligible thermal effects [19]. Their finding that irreversible electroporation can be used as an independent modality for ablation of substantial volumes of tissue was subsequently confirmed in studies on cells [20], small animal models in the liver [21], and on tumors [22] as well as in large animal models in the liver [23] and the heart [24].

Perhaps one of the most important findings of the IRE animal experiments is that the special mode of non-thermal cell ablation has many beneficial effects. For instance, it allows extremely rapid

* Corresponding author. Tel.: +1 540 231 9179; fax: +1 540 231 0970.
E-mail address: davalos@vt.edu (R.V. Davalos).

0017-9310/$ - see front matter © 2008 Elsevier Ltd. All rights reserved.
doi:10.1016/j.ijheatmasstransfer.2008.04.046

Nomenclature

ϕ	electric potential (V)	c_p	heat capacity of tissue (kJ kg^{-1} K^{-1})
σ	electric conductivity (S m^{-1})	σ_0	conductivity of the tissue before electroporation (S m^{-1})
p	Joule heating rate per unit volume (W m^{-3})	V_a	applied voltage (V)
k	thermal conductivity of tissue (W m^{-1} K^{-1})	L	distance between the electrodes (m)
T	temperature above the arterial temperature (°C)	$\tilde{T}$	non-dimensionalized temperature
w_b	blood perfusion term (kg m^{-3} s^{-1})	$\tilde{x}$	non-dimensionalized length
c_b	heat capacity of blood (kJ kg^{-1} K^{-1}	$\tilde{t}$	non-dimensionalized time
q'''	metabolic heat generation (W m^{-3})	$\tilde{q}_0'''$	non-dimensionalized Joule heating term
ρ	tissue density (kg m^{-3})		

regeneration of ablated tissue with healthy tissue [23] without scar formation, and it induces a potentially beneficial immune response [23]. It also allows treatment in the heart [24] and blood vessels [25] without the danger of coagulation in the blood and subsequent emboly. Therefore, the research on IRE presents a new challenge to scientists studying bio-thermal fields. The study of how electrical fields can be applied to living tissue to induce IRE damage to the cell membrane without causing any thermal effects is an emerging area of research. The goal of this study is to introduce the problem to the bio-heat community and illustrate several first order studies in the field.

2. Methods

The heating of the tissue resulting from electroporation can be calculated by adding the Joule heating source term to the Pennes bio-heat transfer equation [26]. The Pennes bio-heat equation is often used to assess the heating associated with each procedure because it can provide an estimate of important biological contributions, such as metabolism and blood flow. As described in [27], the Joule heating source term is evaluated by solving the Laplace equation for the potential distribution associated with an electrical pulse:

$$\nabla \cdot (\sigma \nabla \phi) = 0, \tag{1}$$

where ϕ is the electrical potential and σ is the electrical conductivity of the tissue. The associated Joule heating rate per unit volume, p, from an electric field, is the square of the local electric field, $-\nabla\phi$, times the electrical conductivity of the tissue ($\sigma|\nabla\phi|^2$).

The modified Pennes bio-heat equation has the following form:

$$\nabla \cdot (k \nabla T) - w_b c_b T + q''' + \sigma |\nabla \phi|^2 = \rho c_p \frac{\partial T}{\partial t} \tag{2}$$

where k is the thermal conductivity of the tissue, T is the temperature above the arterial temperature (37 °C), w_b is the blood perfusion, c_b is the heat capacity of the blood, q''' is the metabolic heat generation, ρ is the tissue density, and c_p is the heat capacity of the tissue. It should be noted that the term tissue refers to the aggregate of solid and blood.

Eq. (2) can be non-dimensionalized in a similar fashion as described in [28], which uses the following assumptions: the domain is homogenous, the heat capacity of blood is equal to the tissue ($c_b = c_p = c$) and the metabolic heat generation is negligible.

For irreversible electroporation, the joule heating term is non-dimensionalized by normalizing the electric field with the applied voltage-to-distance ratio:

$$\tilde{q}_0''' = \frac{\sigma E^2}{\sigma_0 (V_a/L)^2} \tag{3}$$

where σ_0 is the conductivity of the tissue before electroporation, V_a is the applied voltage and L is the distance between the electrodes. In the cases where cylindrical or spherical electrodes are used, L is the center-to-center distance between the electrodes. The following additional dimensionless terms are used to non-dimensionalize Eq. (2):

$$\tilde{T} = \frac{Tk}{L^2 \sigma_0 (V_a/L)^2} \tag{4}$$

$$\tilde{x} = \frac{x}{L} \tag{5}$$

$$\tilde{t} = \frac{tk}{\rho c L^2} \tag{6}$$

Expressing Eq. (2) in terms of these non-dimensional quantities for temperature, length, and time reduces it to the following dimensionless form:

$$\nabla^2 \tilde{T} - w_b \frac{cL^2}{k} \tilde{T} + \tilde{q}_0''' = \frac{\partial \tilde{T}}{\partial \tilde{t}} \tag{7}$$

3. Models

Three fundamental models were employed to study the effect of electrode geometries commonly used for IRE on the electric field and the temperature distribution:

Case A: Two 1 mm diameter spheres separated by a distance of 1 cm.
Case B: Two 1 mm diameter cylinders separated by a distance of 1 cm.
Case C: Two infinite plates separated by a distance of 1 cm.

The models were chosen to provide insight, but other configurations can be used as well. It should be noted that these electrode configurations are similar to those commonly used in reversible electroporation. The models are depicted in Fig. 1. For the cylindrical and spherical cases, 1 cm is the center-to-center distance between the electrodes.

For each case, the surface of one electrode is assumed to have a prescribed voltage, and the other electrode is set to ground. Specifically, at the boundary where the tissue is in contact with one electrode:

$$\phi = V_0, \tag{8}$$

where V_0 is the applied voltage, and at the boundary where the tissue is in contact with the other electrode:

$$\phi = 0. \tag{9}$$

The remaining boundaries are treated as electrically insulating:

$$\frac{\partial \phi}{\partial n} = 0. \tag{10}$$

Several thermal boundary conditions can be employed to study the heat exchange between the electrodes and the tissue [27,29,30].

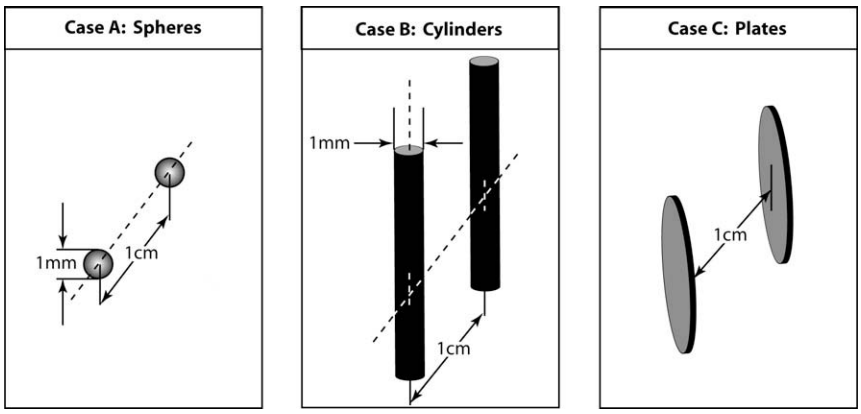

Fig. 1. Models used in study. Case A: two 1 mm diameter spheres separated by a distance of 1 cm. The dashed line indicates the axis of symmetry. Case B: two 1 mm diameter cylinders separated by a distance of 1 cm. The dashed lines indicate the plane of symmetry. Case C: two plates separated by a distance of 1 cm.

However, in this study, the boundaries are taken to be adiabatic at the boundary of the analyzed domain to predict the maximum temperature rise in the tissue:

$$\frac{\partial T}{\partial n} = 0. \tag{11}$$

The spherical and cylindrical cases were solved numerically while the plate electrode configuration was solved analytically. The spherical model and the cylindrical model are 2D models. The spherical case is treated as axis-symmetric and the cylindrical case is treated as symmetric with the plane of symmetry made by the axis of each electrode. The 2D simplification for the needle electrodes implies infinitely long electrodes. This simplification does incur some error, particularly when the ratio of electrode length to electrode gap is small, but it is typically a good approximation for IRE treatment planning. Taking advantage of the geometric symmetry enables avoidance of computationally expensive 3D models.

The values of the tissue heat capacity ($c_p = 4$ kJ kg^{-1} K^{-1}), electrical conductivity ($\sigma = 0.2$ S m^{-1}), thermal conductivity ($k = 0.5$ W m^{-1} K^{-1}), and density ($\rho = 1000$ kg m^{-3}) used in the models are taken from the literature [31,32]. The tissue temperature is assumed to be initially the same as the arterial temperature which is the physiological temperature (37 °C).

The computations were performed with a commercial finite element package (FEMLab, *Comsol AS*, Stockholm, Sweden). The analyzed domain extends far enough from the area of interest (i.e. the area near the electrodes) that the electrically and thermally insulating boundaries at the edges of the domain do not significantly influence the results in the treatment zone.

4. Results and discussion

Fig. 2 shows the electric field distribution and temperature distribution for the spherical case (Case A) and the cylindrical case (Case B) when 1000 V is applied across the electrodes. As described in the model section, only half of the domain is used for the solution to take advantage of the geometrical symmetry.

The surface plots are of the electric field distribution – the dominant parameter dictating which region of tissue has been electroporated [33]. The magnitude of the electric field required to induce IRE is a function of a number of other parameters such as pulse number, pulse length, and tissue type and is an ongoing area of research [22,34,35]. The surface plots reveal that the field distribution is strongly dependent on electrode shape. The results in Fig. 2 show that the electric field distribution decays more gradually in the cylindrical case than in the spherical case. Since the associated Joule heating is strongly dependent on the electric field, the temperature distribution within the tissue is also more visually spread than for the spherical case.

The isotherms show the temperature distribution when the analyzed domain reaches a maximum temperature of 50 °C for an applied pulse. For both geometries, the maximum temperature is at the tissue-electrode interface where the electrodes are in closest proximity to one another. The isotherms are of constant temperatures at 37.1, 37.5, 40, and 45 °C, where the outer curve is 37.1 °C, and the innermost curve (nearest to the electrodes) is 45 °C. For the spherical case, the time required to reach 50 °C (0.000242 s) is an order of magnitude less than the cylindrical electrode case (0.00211 s).

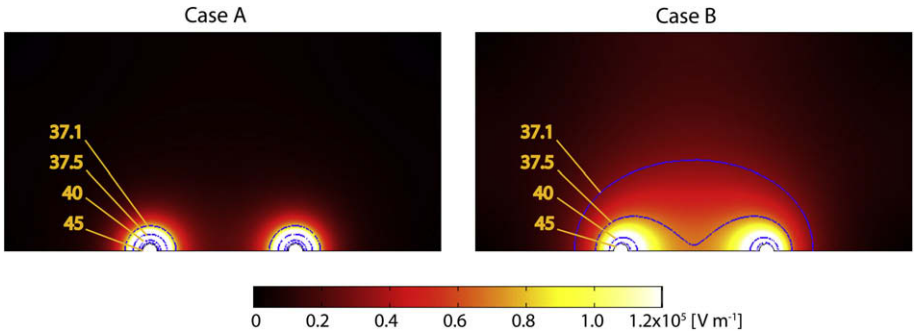

Fig. 2. The electric field and thermal distribution at 1000 V for Case A: two spherical electrodes, and Case B: two cylindrical electrodes. The surface plots show the electric field distribution and the superimposed isotherms show the ensuing temperature distribution when the maximal temperature reaches 50 °C (at 0.000242 s for Case A and 0.00211 s for Case B). The contour lines are 37.1, 37.5, 40, and 45 °C with the highest temperature curve being nearest to the electrode.

The results in Fig. 2 are indicative of the electric field distribution for these two scenarios at any voltage and the solution can be multiplied by a scaling factor to determine the electric field distribution at any other voltage. For example, the electric field for 500 V and 2000 V can be determined by multiplying the values on the scale bar by 1/2 or 2, respectively.

Fig. 3 shows the temperature distribution along the axis of symmetry for the two-sphere electrode case and the two-cylinder electrode case when 2000 V is applied across the electrodes. The temperature profiles shown are when the maximal temperature approaches 40, 45, and 50 °C, respectively. The maximum temperature in the tissue approaches these temperatures at pulse durations of 0.0000119, 0.0000318, and 0.0000516 s, respectively, for the two-spherical electrode case and pulse durations of 0.000116, 0.000313, and 0.000510 s, respectively, for the two-cylindrical electrode case.

Fig. 3 confirms our results in Fig. 2; the temperature distribution within the tissue decays quickly from the electrode surface and that the drop off is more pronounced with the spherical case. Also in agreement with our results in Fig. 2 is that the pulse dura-

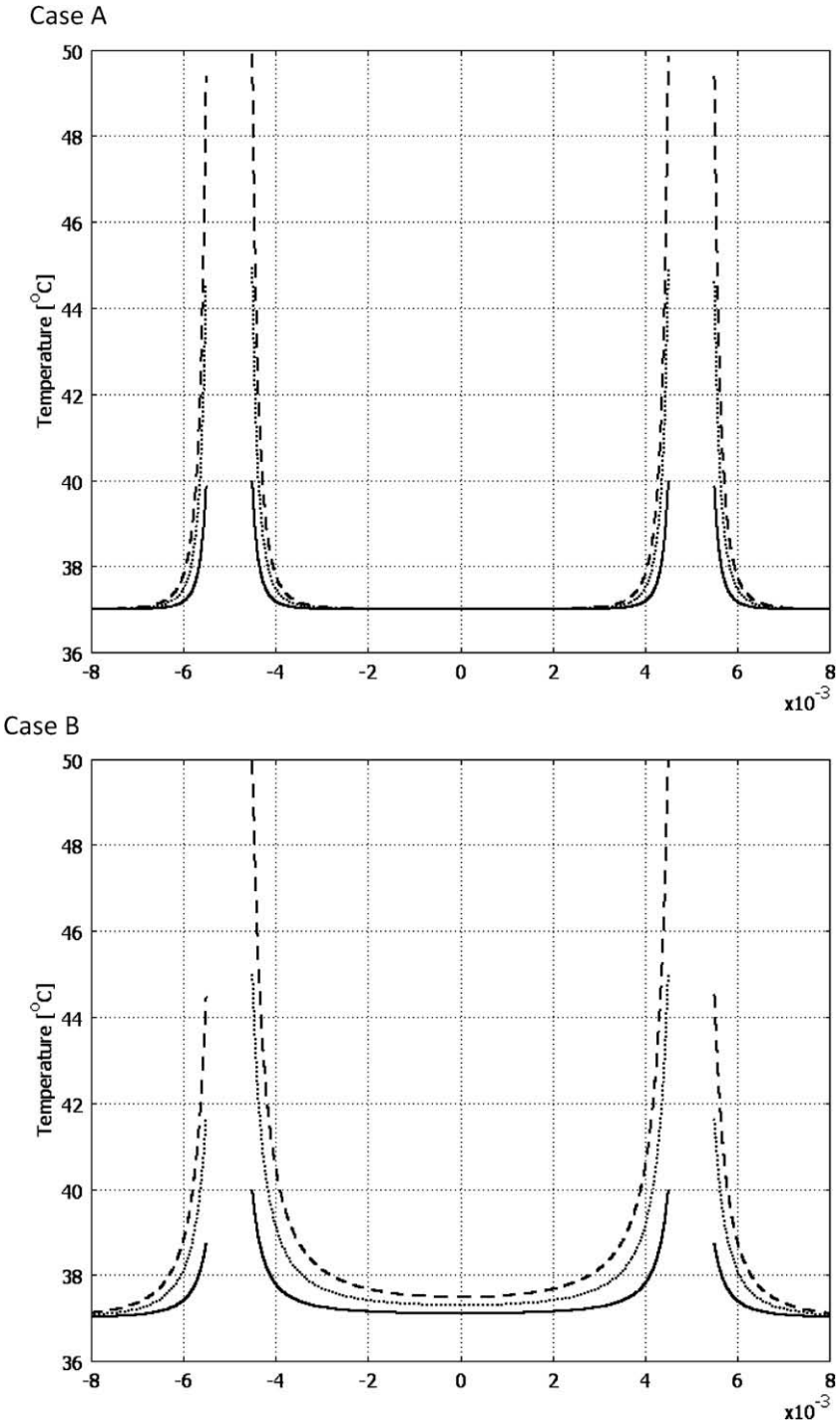

Fig. 3. Temperature distribution along cross section when the maximal temperature in the domain approaches 40, 45 and 50 °C when 2000 V is applied across Case A: the two spherical electrodes and Case B: the two cylindrical electrodes. Cross-sectional line is along the line of symmetry of the two models.

tion required to reach a maximal temperature within the tissue domain is consistently one tenth for the spherical electrode case than for the cylindrical case. It should also be noted that the boundary at the electrode interface was treated as thermally insulating and that heat conduction through the electrodes was not considered. Therefore, these results are conservative [22,27].

Fig. 4 shows the maximum temperature within the tissue as a function of pulse duration normalized for generality for the three cases described in this study. The temperature is normalized by the applied voltage-to-distance ratio as well as other properties as described in the methods, but it should be noted that a number of other factors such as electrode diameter could have been used. These plots were obtained by calculating the pulse duration required to reach a maximal temperature of 40, 45, and 50 °C for an applied voltage of 500, 1000, or 2000 V for each case. At a specified voltage, the solutions are perfectly linear (i.e., $R^2 = 1$) for each of the three geometries. Therefore, these solutions can be extrapolated to determine the required pulse duration to stay below a specified temperature using the applied voltage for each electrode configuration. For example, pulse durations on the order of 100 μs are normally used for therapeutic electroporation, and such pulse lengths have been shown to be highly effective for tumor ablation using IRE [22]. Fig. 4 can be used to obtain the maximum voltage allowable to stay below a certain temperature limit when a 100 μs is applied.

Since thermal damage is a function of temperature and duration, the negligible heating associated with these case studies is emphasized by the fact that an electroporation pulse is a very small fraction of a second long. The models presented in this study show the temperature distribution due to an electroporation pulse and methods to calculate the thermal dose or damage associated with a procedure can be found in [22,30,36].

This fundamental study highlights some of the basic results from an electroporation procedure. However, there are many complexities that may need to be considered when creating models which were not within the scope of this study. An example includes the fact that properties of tissue, such as thermal and electrical conductivities, are functions of temperature [37]. Their dependence can be found in the literature and incorporated into future models if necessary. Furthermore, the electrical conductivity of tissue during electroporation increases as a result of electroporation [38–41]. Even though such changes were not incorporated into the present model, such changes could be important especially, if the tissue is heterogeneous. These changes can be readily incorporated into numerical models [40,42]. An advantage of the fact that the impedance changes during IRE is that it provides an active means for the physician to monitor the procedure and image which tissue region has been irreversibly electroporated [39,42,43].

The blood diffusion was assumed to be zero since it was shown to have a negligible effect in the short time span of an electroporation pulse [27]. Furthermore, it may be possible to neglect blood flow since results in [21] suggest that perfusion stops during IRE, which may assist in inducing total necrosis of the tissue. Nevertheless, it may be necessary to consider when multiple pulses are used with long delays between the pulses.

The application of a short electroporation pulse across needle electrodes will cause a sudden deposition of a highly non-uniform amount of thermal energy [21]. Immediately after the pulse (and to some extent during the pulse), this thermal energy will begin to diminish in strength as it spreads throughout the tissue as described by the heat diffusion equation. This heating is so non-uniform that points far from the electrode surface are not subjected to the more intense heating which occurs near the electrodes until some time has passed.

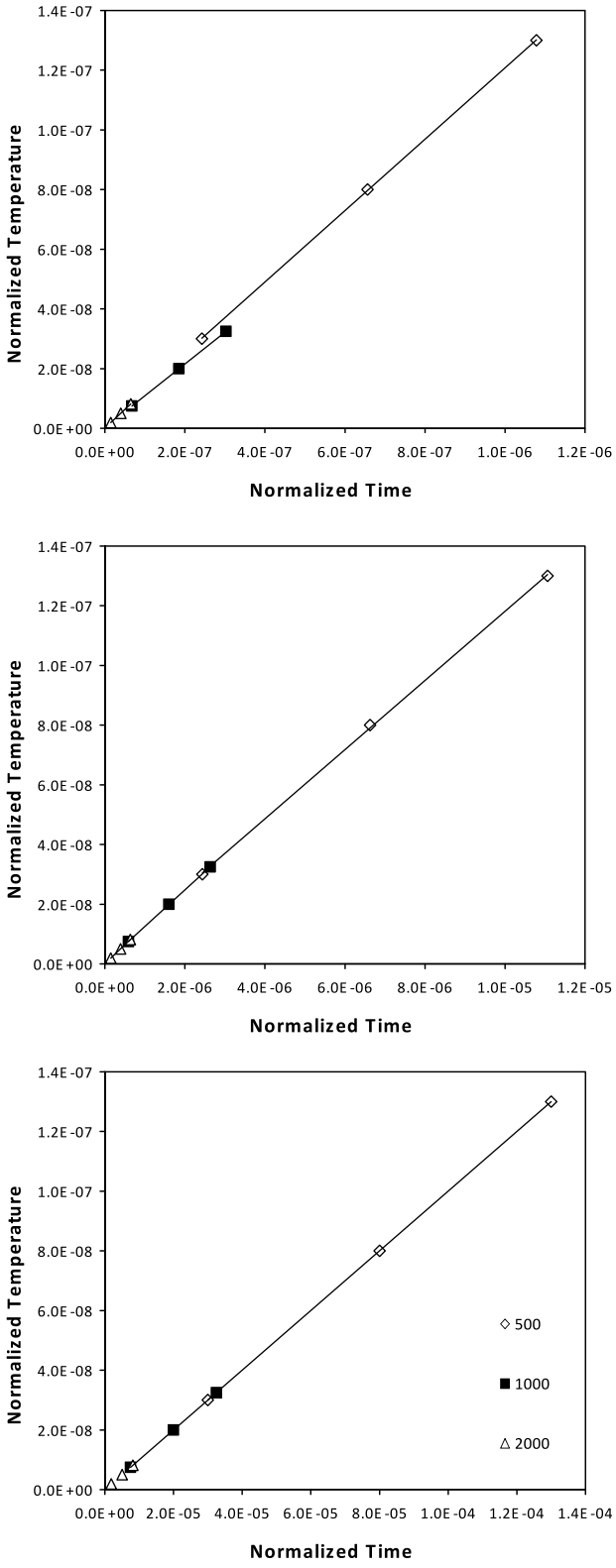

Fig. 4. Non-dimensionalized plot of temperature vs. time depicting the duration required to reach a maximal temperature of 40, 45 and 50 °C when 500, 1000 or 2000 V are applied for: (a) two-spheres, (b) two cylinders, and (c) two plates.

5. Conclusion

In order to design protocols for an IRE procedure, the electric field distribution must be determined, which is dependent on the

procedure's specific electrode geometry and tissue impedance distribution. By predicting the electric field distribution for a specific scenario, the electrode geometry can be optimized to ablate the entire targeted region while minimally affecting the surrounding tissue. Furthermore, to verify that a specific protocol does not induce thermal effects, the temperature distribution can be calculated from the electric field distribution, the electric pulse parameters, and tissue properties.

The goal of this work was to introduce the relatively new field of IRE to the bio-heat transfer community. Three fundamental models, which are typical electrode configurations employed in IRE, were used to illustrate some basic effects of electrode geometry and voltage parameters on the resulting temperature distribution.

References

[1] E. Neumann, M. Schaefer-Ridder, Y. Wang, P.H. Hofschneider, Gene transfer into mouse lyoma cells by electroporation in high electric fields, J. EMBO 1 (1982) 841–845.

[2] U. Zimmermann, Electric field-mediated fusion and related electrical phenomena, Biochim. Biophys. Acta (BBA) 694 (1982) 227–277.

[3] S. Orlowski, J.J. Behradek, C. Paoletti, L.M. Mir, Transient electropermeabilization of cells in culture. Increase in the cytotoxicity of anticancer drugs, Biochem. Pharmacol. 37 (1988) 4724–4733.

[4] M. Okino, H. Mohri, Effects of a high-voltage electrical impulse and an anticancer drug on in vivo growing tumors, Jpn. J. Cancer Res. 78 (1987) 1319–1321.

[5] L.M. Mir, M. Belehradek, C. Domenge, B. Luboniski, S. Orlowski, J. Belehradek, B. Schwaab, B. Luboniski, C. Paoletti, Electrochemotherapy, a novel antitumor treatment: first clinical trial, C.R. Acad. Sci. III (1991) 313.

[6] A.V. Titomirov, S.I. Sukharev, E. Kristanova, In vivo electroporation and stable transformation of skin cells of newborn mice by plasmid DNA, Biochim. Biophys. Acta 1088 (1991) 131–134.

[7] D.C. Chang, B.M. Chassy, J.A. Saunders, A.E. Sowers, Guide to Electroporation and Electrofusion, Academic Press, Inc., San Diego, CA, 1992.

[8] S.B. Dev, D.P. Rabussay, G. Widera, G.A. Hofmann, Medical applications of electroporation, IEEE Trans. Plasma Sci. 28 (February) (2000) 206–223.

[9] R. Heller, R. Gilbert, M.J. Jaroszeski, Clinical applications of electrochemotherapy, Adv. Drug Deliv. Rev. 35 (1999) 119–129.

[10] D. Miklavcic, M. Puc, Electroporation, in: Wiley Encyclopedia of Biomedical Engineering, John Wiley & Sons, New York, 2006.

[11] E. Neumann, A.E. Sowers, C.A. Jordan, Electroporation and Electrofusion in Cell Biology, Plenum Press, New York, NY, 1989.

[12] L.M. Mir, Therapeutic perspectives of in vivo cell electropermeabilization, Bioelectrochemistry 53 (2001) 1–10.

[13] M.J. Jaroszeski, R. Gilbert, C. Nicolau, R. Heller, In vivo gene delivery by electroporation, Adv. Appl. Electrochem. 35 (1999) 131–137.

[14] M. Prausnitz, S. Mitragotri, R. Langer, Current status and future potential of transdermal drug delivery, Nat. Rev. Drug Discov. 3 (2004) 115–124.

[15] J.C. Weaver, Y.A. Chizmadzhev, Theory of electroporation: a review, Bioelectrochem. Bioenerg. 41 (1996) 135–160.

[16] J. Teissie, M. Golzio, M.P. Rols, Mechanisms of cell membrane electropermeabilization: a minireview of our present (lack of ?) knowledge, Biochem. Biophys. Acta 1724 (2006) 270–280.

[17] U. Zimmermann, G. Pilwat, F. Beckers, F. Riemann, Effects of external electrical fields on cell membranes, Bioelectrochem. Bioenerg. 3 (1976) 58–83. 3, pp. 58–83..

[18] B. Rubinsky, Irreversible Electroporation in Medicine, Technol. Cancer Res. Treatment 6 (2007) 255–260.

[19] R.V. Davalos, L.M. Mir, B. Rubinsky, Tissue ablation with irreversible electroporation, Ann. Biomed. Eng. 33 (2005) 223–231.

[20] L. Miller, J. Leor, B. Rubinsky, Cancer cells ablation with irreversible electroporation, Technol. Cancer Res. Treatment 4 (2005) 699–706.

[21] J.F. Edd, L. Horowitz, R.V. Davalos, L.M. Mir, B. Rubinsky, In vivo results of a new focal tissue ablation technique: irreversible electroporation, IEEE Trans. Biomed. Eng. 53 (2006) 1409–1415.

[22] B. Al-Sakere, F. André, C. Bernat, E. Connault, P. Opolon, R.V. Davalos, B. Rubinsky, L.M. Mir, Tumor ablation with irreversible electroporation, PLoS ONE 2 (November) (2007) e1135:1–e1135:8.

[23] B. Rubinsky, G. Onik, P. Mikus, Irreversible electroporation: a new ablation modality – clinical implications, Technol. Cancer Res. Treatment 6 (2007) 37–48.

[24] J. Lavee, G. Onik, P. Mikus, B. Rubinsky, A novel non-thermal energy source for surgical epicardial atrial ablation: irreversible electroporation, Heart Surg. Forum 10 (April) (2007) E162–E167.

[25] E. Maor, A. Ivorra, J. Leor, B. Rubinsky, The effect of irreversible electroporation on blood vessels, Technol. Cancer Res. Treatment 6 (2007) 307–312.

[26] H.H. Pennes, Analysis of tissue and arterial blood temperatures in the resting forearm, J. Appl. Physiol. 1 (1948) 93–122.

[27] R.V. Davalos, B. Rubinsky, L.M. Mir, Theoretical analysis of the thermal effects during in vivo tissue electroporation, Bioelectrochemistry 61 (2003) 99–107.

[28] K.R. Foster, A. Lozano-Nieto, P.J. Riu, Heating of tissues by microwaves: a model analysis, Bioelectromagnetics 19 (1998) 420–428.

[29] S.M. Becker, A.V. Kuznetsov, Numerical modeling of in vivo plate electroporation thermal dose assessment, J. Biomech. Eng. 128 (Feb) (2006) 76–84.

[30] S.M. Becker, A.V. Kuznetsov, Thermal damage reduction associated with in vivo skin electroporation: a numerical investigation justifying aggressive pre-cooling, Int. J Heat Mass Transfer 50 (2007) 105–116.

[31] Z.S. Deng, J. Liu, Blood perfusion-based model for characterizing the temperature fluctuations in living tissue, Phys. Stat. Mech. Appl. 300 (2001) 521–530.

[32] A. Swarup, S. Stuchly, A. Surowiec, Dielectric properties of mouse MCA1 fibrosarcoma at different stages of development, Bioelectromagnetics 12 (1991) 1–8.

[33] D. Miklavcic, K. Beravs, D. Semrov, M. Cemazar, F. Demsar, G. Sersa, The importance of electric field distribution for effective in vivo electroporation of tissues, Biophys. J. 74 (1998) 2152–2158.

[34] B. Al-Sakere, C. Bernat, F. Andre, E. Connault, P. Opolon, R.V. Davalos, L.M. Mir, A study of the immunological response to tumor ablation with irreversible electroporation, Technol. Cancer Res. Treatment 6 (2007) 301–306.

[35] G. Onik, P. Mikus, B. Rubinsky, Irreversible electroporation: implications for prostate ablation, Technol. Cancer Res. Treatment 6 (2007) 295–300.

[36] J.F. Edd, R.V. Davalos, Mathematical modeling of irreversible electroporation for treatment planning, Technol. Cancer Res. Treatment 6 (2007) 275–286.

[37] F.A. Duck, Physical Properties of Tissues: A Comprehensive Reference Book, Academic Press, San Diego, 1990.

[38] M. Pavlin, D. Miklavcic, Effective conductivity of a suspension of permeabilized cells: a theoretical analysis, Biophys. J. 85 (2003) 719–729.

[39] R.V. Davalos, D.M. Otten, L.M. Mir, B. Rubinsky, Electrical impedance tomography for imaging tissue electroporation, IEEE Trans. Biomed. Eng. 51 (2004) 761–767.

[40] D. Miklavcic, D. Sel, D. Cukjati, D. Batiuskaite, T. Slivnik, L.M. Mir, Sequential finite element model of tissue electropermeabilisation, in: Proceedings of the 26th Annual International Conference of the IEEE EMBS, San Francisco, CA, 2004.

[41] R.C. Lee, D. Zhang, J. Hannig, Biophysical injury mechanisms in electrical shock trauma, in: M.L. Yarmish, K.R. Diller, M. Toner (Eds.), Ann. Rev. Biomed. Eng., vol. 2, Annual Review Press, Palo Alto, 2000, pp. 477–509.

[42] R.V. Davalos, D.M. Otten, B. Rubinsky, A feasibility study for electrical impedance tomography as a means to monitor tissue electroporation for molecular medicine, IEEE Trans. Biomed. Eng. 49 (April) (2002) 400–403.

[43] E.W. Lee, C.T. Loh, S.T. Kee, Imaging guided percutaneous irreversible electroporation: ultrasound and immunological correlation, Technol. Cancer Res. Treatment 6 (2007) 287–294.